Role of cyclic process in the initial stage of diamond deposition during bias enhanced nucleation

Y. Hayashi,[a] Y. Matsushita, T. Soga, M. Umeno, and T. Jimbo
Department of Environmental Technology and Urban Planning, Nagoya Institute of Technology, Gokiso-cho, Showa-ku, Nagoya 466-8555, Japan

(Received 26 June 2001; accepted for publication 1 April 2002)

The initial nucleation of diamond film on a Si substrate, deposited by a three-step growth process together with a cycle bias enhanced nucleation (BEN) growth/H_2 plasma etching technique in a microwave plasma enhanced chemical vapor deposition system has been investigated by atomic force microscopy, Raman spectroscopy and x-ray photoelectron spectroscopy. The surface morphology and the uniformity of {100}-oriented textured grains at the BEN step were found to be greatly increased by applying the cyclic process with some optimal H_2 plasma etching time during the BEN stage. © *2002 American Institute of Physics.* [DOI: 10.1063/1.1480116]

I. INTRODUCTION

The formation of a large-area, possibly single-crystalline chemical vapor deposition (CVD) heteroepitaxial diamond film on a Si substrate has long been viewed as a promising system for semiconductor device application such as ultraviolet (UV) light sources and metal–semiconductor field effect transistors (MISFETs). In order to develop industrial products, many problems which occur during the growth process must be resolved.

Many researchers have been working on the development of heteroepitaxial diamond growth on a Si substrate with the aim of establishing technologies to realize large-area single crystal diamond. Bias enhanced nucleation (BEN) was developed by Yugo *et al.*[1] and later adopted by Stoner *et al.*[2] to obtain diamond film with a {100}-oriented texture on a Si(100) substrate, where high nucleation density can be achieved ($\sim 10^{10}$ cm^{-2}). Wolter *et al.*[3] have further added a carburization step before applying the BEN process, resulting in a large percentage of the diamond grains having a {100} orientation on the Si(100) substrate. So far, two deposition techniques have been introduced to obtain high quality heteroepitaxial diamond film on Si: one is a two-step process (BEN→growth)[4] and the other is a three-step process (carburization → BEN → growth).[1] The carburization step forms an *in situ* carbide conversion layer on Si, and thus the nucleation/incubation period can be reduced at the BEN step.[3] In recent years, application of a cyclic process (modulation of the etching process by a combination of BEN and H_2 plasma etching) during the BEN stage in the three-step method has been reported to increase the deposition rate and to improve the film quality.[5–8]

Although the cyclic process has been studied by many researchers using scanning electron microscopy (SEM) of large areas,[3,4,7,8] there has been no detailed investigation of the role of H_2 plasma on the evolution of the film surface at the BEN step of diamond deposition on a Si substrate by atomic force microscopy (AFM). In this work, we investigate the effect of a cyclic technique on the initial BEN stages of diamond film deposition by microwave plasma enhanced chemical vapor deposition (MPECVD). The films are characterized by AFM, Raman spectroscopy and x-ray photoelectron spectroscopy (XPS).

II. EXPERIMENT

The diamond films were deposited in a 2.45 GHz Applied Science and Technology (ASTeX, US), MPECVD system. The mirror-polished Si(100) substrates, pretreated in an aqueous solution of HF (HF:H_2O=1:1 by volume) to remove oxide, were set on a molybdenum (Mo) holder. Then they were cleaned with H_2 plasma for 20 min at 900 °C. The diamond films were deposited through a three-step process. Carburization of the substrate was carried out at a substrate temperature of 800 °C and at a microwave power of 1200 W for 1 h in a range of CH_4/H_2 gas mixtures at 40 Torr. During the BEN stage, a negative dc bias voltage (−250 V) was applied to the substrate through the back side of the Mo holder. The substrate temperature, microwave power, and total pressure were maintained at 750 °C, 1000 W, and 25 Torr, respectively. For the cyclic process, a mixture of 2% CH_4 in H_2 plasma (the BEN process) and H_2 plasma etching (the etching process) were sequentially applied during the BEN stage by switching of the CH_4 flow rate on/off. The film deposition conditions are summarized in Table I.

The surface morphological features of the diamond films in the nucleation stage were examined by a Seiko Instruments SPI-3800N AFM system. The quality and bonding configuration were characterized by Raman spectroscopy and XPS, respectively. The Raman spectra were measured in back-scattering geometry using the 514.5 nm line of an Ar^+ ion laser at room temperature in the spectral range from 900 to 1800 cm^{-1} with a resolution of 1.0 cm^{-1}, and the signals were separated by a 80 cm monochromator. The XPS measurements employed Al K_α radiation ($h\nu$=1486.6 eV) with a 600 μm spot size and were carried out to analyze bonding configurations in the carbon network. The XPS spectra of the films were obtained after a sputter cleaning using 1.5 keV

[a]Electronic mail: yhayashi@theo.elcom.nitech.ac.jp

 © 2002 American Institute of Physics

Downloaded 23 Aug 2010 to 133.68.192.97. Redistribution subject to AIP license or copyright; see http://jap.aip.org/about/rights_and_permissions

TABLE I. Summary of the carburization and BEN conditions and average grain sizes measured in a 5×5 μm^2 area.

Sample	Carburization step CH_4/H_2 (%)	BEN step (BEN/H_2 plasma etching)	Average grain size (nm)
Carb-1	1	⋯	110
Carb-2	2	⋯	105
Carb-3	3	⋯	135
BEN-nocyc-15-0	2	15/0 min	167
BEN-cyc-5-5	2	5/5 min	300
BEN-cyc-5-10	2	5/10 min	205

Ar^+ ion beam for 10 s in order to remove surface contaminants. It is well known that Ar^+ ion sputtering modifies some surface diamond carbon to graphite. In our experiments, we did not observe any change of structure of the films by Ar^+ ion sputtering with beam energies up to 3.0 keV.

III. RESULTS AND DISCUSSION

We first investigated in detail the surface morphology of the sample after the carburization step since the surface morphology after the BEN step reflects the roughness of the carburized substrate. The AFM average roughness (*Ra*) and root mean square (rms) roughness decreased from 1.6 and 1.2 nm to 1.4 and 1.0 nm, respectively, as the CH_4 concentration is increased from 1% to 2%, as shown in Fig. 1. However, both *Ra* and the rms again increase as the CH_4 concentration is increased above 2%. This indicates that there is some optimal CH_4 concentration at around 2% during the carburization stage.

We have observed that the surface morphologies of the samples which were treated with the cyclic process during the carburization stage are clearly different from the sample without the cyclic process. Figure 2 shows three-dimensional AFM images scanned in a 1×1 μm^2 microarea of the surface after the BEN step. We note that the total BEN time, without the H_2 plasma etching time, we set to 15 min in this experiment. As shown in Fig. 2(a), the columnar or cone shaped diamond, with both diameter and height of around 200 nm, initially nucleates randomly on the Si substrate of the sample without the cyclic process (BEN-nocyc15-0). This random nucleation is due to the random amorphous carbon (*a*-C) or sp^2 bonded carbon layer created during carburization. The diamond nuclei cannot be grown on these layers, which can be transformed into sp^3 bonded carbon or many remain sp^2 bonded carbon in a future diamond growing process, at this stage. For the sample BEN-cyc-5-5 where the process has been carried out three times with a BEN/H_2 plasma etching time ratio of 5 min/5 min, we clearly find as shown in Fig. 2(b) the high uniformity of the trapezoidal shaped diamond crystallites, 300 nm square and 100 nm high, which are con-

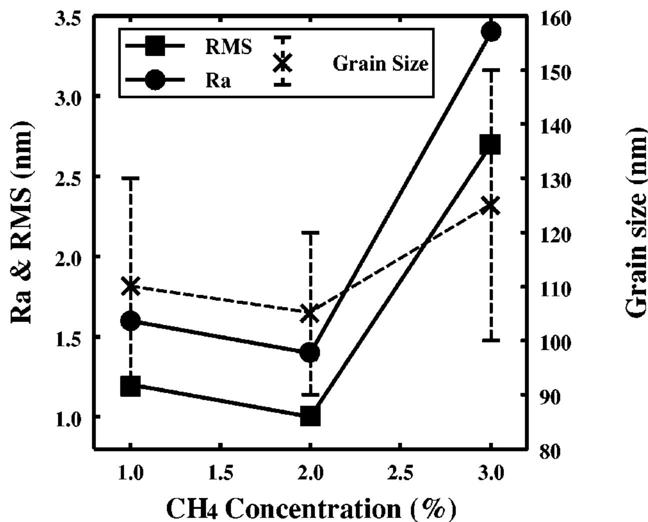

FIG. 1. Plot of the AFM average roughness (*Ra*) and rms roughness as well as the average grain size (5×5 μm^2 area) after the carburization step as a function of the CH_4 concentration.

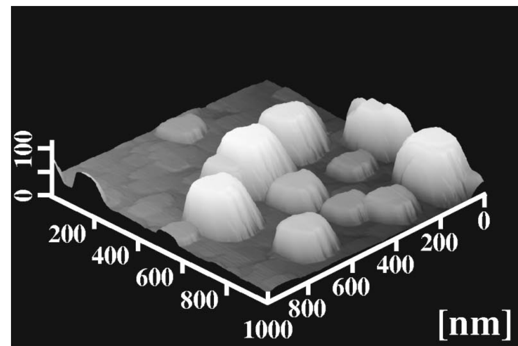

(a)

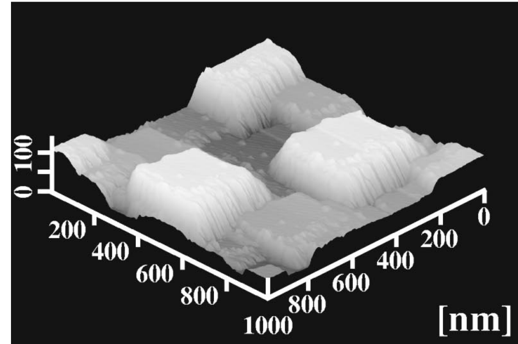

(b)

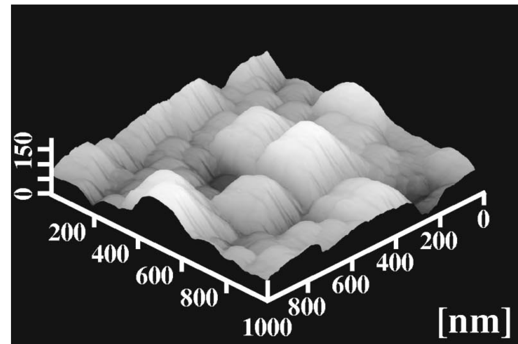

(c)

FIG. 2. Three-dimensional AFM surface morphologies scanned in a 1×1 μm^2 area after the BEN step (a) without the cyclic process and (b), (c) with the cyclic process. The nucleation/etching time ratios are 5/5 min and 5/10 min for AFM images (b) and (c), respectively.

Downloaded 23 Aug 2010 to 133.68.192.97. Redistribution subject to AIP license or copyright; see http://jap.aip.org/about/rights_and_permissions

nected to each other and enhance the alignment of the nuclei. In other words, a high density (or coverage) of {100}-oriented, textured grains has been obtained.

Recently, a similar result was reported by Zhang and Jiang,[9] where they found improvement of the diamond film orientation by applying H^+ ion etching after the BEN step. With an increase in etching time up to 10 min at the cyclic process, we can still observe the trapezoidal shape, 100 nm square and 150 nm high, in sample BEN-cyc-5-10, as shown in Fig. 2(c). However, the surface morphology is gradually etched out of the trapezoidal shape and some of the diamond crystallites have become pyramidal or cone shaped. Moreover, the surface roughness increased and the size is less uniform.

In order to investigate the effect of H_2 plasma etching time on the surface morphology, we extended the etching time to more than 10 min and the surface morphology was found to further worsen. Therefore, our experiment clearly shows that the surface morphology sensitively depends on the H_2 plasma ion etching time in the cyclic process. It should be noted that the number of hydrogen ions bombarding the Si substrate and the degree of ionization of the plasma, which are strongly correlated to the etching efficiency, are changed by the negative substrate bias condition. Thus the H_2 plasma etching time depends on the BEN condition. It is known that atomic hydrogen and hydrogen ions (H^+) etch sp^2 bonded carbon and graphite at a faster rate than sp^3 bonded carbon.[10] The morphological evolution observed by AFM indicates that hydrogen ions in the H_2 plasma remove the sp^2 carbon present in the sp^3 carbon network, thereby increasing the number of available sites for further growth of sp^3 carbon or diamond nuclei.[11]

We also measured three-dimensional AFM images scanned in a $5\times5\ \mu m^2$ wide area of the surfaces of samples BEN-nocyc-15-0 and BEN-cyc-5-5 without and with the cyclic process, respectively. Sample BEN-nocyc-15-0 shows that the pyramidal or cone shaped particles formed randomly over the surface. In the case of sample BEN-cyc-5-5, however, most of the particles are of uniform size with trapezium shape and are well oriented relative to the Si(100) surface.

Raman spectroscopy was performed in order to obtain information on the surface quality of the films deposited with only carburization and with the cyclic process. As shown in Fig. 3, the Raman spectrum for the sample deposited without the cyclic process (BEN-nocyc-15-0) shows three Raman bands at ~960, 1140, and 1555 cm^{-1}. The first Raman band indicates the coexistence of the second-order transverse optical (TO) phonon of Si substrate at 960 cm^{-1} and the silicon carbide (SiC) A_1 longitudinal optical (LO) phonon at 967 cm^{-1}. It is interesting to note that the peak at around 1140 cm^{-1}, which is assumed to originate from the nanocrystalline form of diamond,[12] indicates that the nondiamond carbon precursors are incorporated into the diamond microparticles at the initial stage of BEN.[13] The origin of the last peak near 1555 cm^{-1} is attributed to microcrystalline graphite or amorphous carbon.[14] The main function of carburization is probably to provide microcrystalline graphite on the Si surface which might act as a precursor for SiC formation. The details will be discussed later. Figures 3(c) and 3(d) show Raman

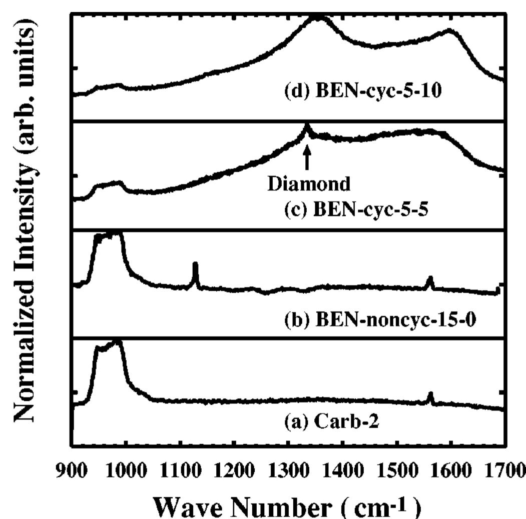

FIG. 3. First order Raman spectra of the samples after (a) the carburization step (Carb-2), (b) the BEN step without the cyclic process, and (c),(d) the BEN step with the cyclic process. The nucleation/etching time ratios are 5/5 min and 5/10 min for spectra (c) and (d), respectively.

spectra for samples BEN-cyc-5-5 and BEN-cyc-5-10, respectively, deposited for different H_2 plasma etching times at the cyclic process. Two broader strong peaks corresponding to disordered diamond (the D band) (around 1360 cm^{-1}) and graphite (the G band) (around 1580 cm^{-1}) were found in samples 4 and 5, which indicates the presence of both graphitic and disordered sp^2 carbon. We have observed a well-defined first order diamond peak (1332 cm^{-1}) in sample BEN-cyc-5-5 but no diamond peak in sample BEN-cyc-5-10 at this stage. This result clearly indicates that the Raman diamond peak is sensitive to the different surface morphologies of initial grains that evolved with different BEN/H_2 plasma etching conditions. As discussed above, the morphology and uniformity of {100}-oriented textured initial grains of sample BEN-cyc-5-5 degrade with an increase in H_2 plasma etching time (sample BEN-cyc-5-10). Therefore, there is some optimal BEN/H_2 plasma etching condition. The peak intensity at ~960 cm^{-1} greatly decreases with the introduction of the cyclic process, although the total BEN time is same. This may be due to enhancement of the coverage of diamond or/and diamond-like carbon on Si substrates, as observed from the AFM images shown in Fig. 2.

Figure 4 shows the change in the C_{1s} of XPS spectra for samples Carb-2, BEN-nocyc-15-0, BEN-cyc-5-5 and BEN-cyc-5-10. The spectral peak intensities are normalized to the maximum peak intensity. Each spectrum consists of two peaks that can be approximately fitted by a superposition of two Gaussian distribution curves at around 283.1 and 284.9 eV. The former is attributed to silicon carbide (SiC) and the latter to diamond (C-C).[15] For sample Carb-2 after the carburization step, the film surface that formed is mainly SiC which may be amorphous.[9] The intensity ratio of the diamond and SiC peak, $I_{\text{C-C}}/I_{\text{SiC}}$, increases after applying the BEN step. This indicates that the amount of carbon layer on the surface increases due to an increase of impinging carbonaceous ions at BEN. Although the total BEN time was the same, 15 min, in this experiment, the $I_{\text{C-C}}/I_{\text{Si-C}}$ markedly

Downloaded 23 Aug 2010 to 133.68.192.97. Redistribution subject to AIP license or copyright; see http://jap.aip.org/about/rights_and_permissions

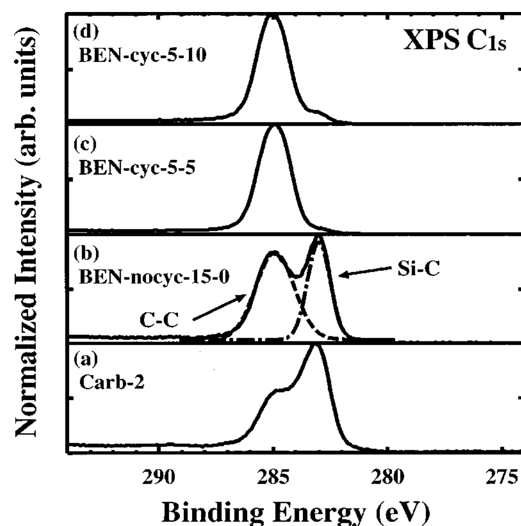

FIG. 4. XPS C_{1s} core-level spectra of the samples after (a) the carburization step (Carb-2), (b) the BEN step without the cyclic process, and (c),(d) the BEN step with the cyclic process. The nucleation/etching time ratios are 5/5 min and 5/10 min for spectra (c) and (d), respectively.

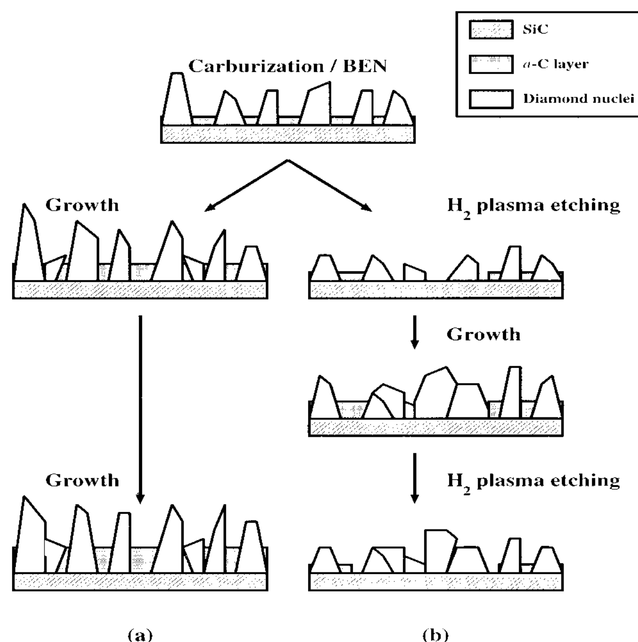

FIG. 5. Schematic diagram of the models of the initial stage of diamond deposition during the BEN step (a) without the cyclic process and (b) with the cyclic process.

increased by applying the cyclic process during the BEN stage. It is suggested that the C-C bonds are enhanced by H_2 plasma etching and that diamond nuclei are formed. As for the increase of $I_{C\text{-}C}/I_{Si\text{-}C}$, it is also probably growth of the diamond film and thus obscureness of the substrate that leads to the reduction of the SiC phonon in the Raman spectra and the increased $I_{C\text{-}C}/I_{Si\text{-}C}$ XPS ratio. Moreover, this is because some of the amorphous SiC and silicon dioxide (SiO_2), which are hidden in the diamond grain boundaries, is removed by H_2 plasma etching during the BEN.[16] This tendency correlates well with the Raman results.

The growth sequence of the BEN without and with the cyclic process can be explained by the schematics, as shown in Figs. 5(a) and 5(b). Both diamond growth and H_2 plasma etching of *a*-C and carbon atoms from the diamond surface occur during the BEN stage without the cyclic process simultaneously, such as sample BEN-nocyc-15-0. Although secondary nucleation cannot be formed on *a*-C, the average grain size may increase due to the redeposition process but growth of the grains is very slow. And the distribution of the grains is not uniform. These result in a microstructure consisting of only columnar small grains isolated from each other by *a*-C's [Fig. 5(a)]. In contrast, the extensive etching of *a*-C and carbon atoms from the diamond surface is accelerated in H_2 plasma, such as for sample BEN-cyc-5-5. Therefore, the *a*-C is etched off completely in some regions. The etching efficiency of H^+ ions is lower on (100) faces than that on other faces due to the very low atom density of the (100) face.[9,17,18] This selective etching caused by H^+ ion enhances the surface morphology in a trapezoidal shape. After another deposition, the grains or secondary nucleations are connected or overlapped by each other and {100}-textured diamond can be deposited on {100}-oriented grains. Therefore, the grain size increases and distribution of the grains is uniform [Fig. 5(b)]. In the case of sample BEN-cyc-5-10, however, the longer H_2 etching time leads to a no longer trapezoidal shape and a decrease in grain size. The variation of the average grain sizes at the BEN step, listed in Table I, therefore reflects the BEN/H_2 plasma etching time ratio.

IV. SUMMARY AND CONCLUSION

We have investigated the effect of the cyclic process in the three-step growth method on the initial nucleation stage of diamond film on a Si(100) substrate deposited by MPECVD. As observed for sample BEN-cyc-5-5 by AFM morphological evolution, the number of oriented {100}-textured grains and the overall coverage of the film can be greatly increased by applying the cyclic process with some optimal H_2 plasma etching time during the BEN stage. Raman and XPS results indicate that the SiC and *a*-C layers are formed by the carburization step and then nondiamond components such as amorphous SiC and/or *a*-C layers are removed by the hydrogen ions in the H_2 plasma at the cyclic process, resulting in the morphological change of textured {100} surface observed by AFM.

ACKNOWLEDGMENTS

The authors would like to acknowledge Dr. Md. M. Rahman and Dr. P. M. Sirimanne for useful discussions. This work was partly supported by the Japan Society for the Promotion of Science under the program "Research for the Future."

[1] S. Yugo, T. Kanai, T. Kimura, and T. Mito, Appl. Phys. Lett. **58**, 1036 (1991).
[2] B. R. Stoner, G.-H. M. Ma, S. D. Wolter, and J. T. Glass, Phys. Rev. B **45**, 11067 (1992).
[3] S. D. Wolter, B. R. Stoner, J. T. Glass, D. S. Buhaenko, C. E. Jenkins, and P. Southworth, Appl. Phys. Lett. **62**, 1215 (1993).
[4] X. Jiang, C.-P. Klages, R. Zachai, M. Hartweg, and H.-J. Fusser, Appl. Phys. Lett. **62**, 3438 (1993).

Downloaded 23 Aug 2010 to 133.68.192.97. Redistribution subject to AIP license or copyright; see http://jap.aip.org/about/rights_and_permissions

[5] D. S. Olson, M. A. Kelly, S. Kapoor, and S. B. Hagstormer, J. Mater. Res. **9**, 1546 (1994).
[6] S. H. Kim, Y. S. Park, I. T. Han, W. S. Yun, and J.-W. Lee, Thin Solid Films **290–291**, 161 (1996).
[7] S. H. Kim, Y. S. Park, W. S. Yun, and J.-W. Lee, J. Cryst. Growth **180**, 198 (1997).
[8] J.-W. Lee, S. H. Kim, Y. S. Park, and I.-T. Han, Thin Solid Films **303**, 264 (1997).
[9] W. J. Zhang and X. Jiang, Thin Solid Films **303**, 84 (1999).
[10] S. Yugo, T. Kanai, and T. Kimura, Diamond Relat. Mater. **1**, 388 (1992).
[11] M. Frenklach and H. Wang, Phys. Rev. B **43**, 1520 (1991).
[12] R. J. Nemanich, J. T. Glass, G. Lucovsky, and R. E. Shroder, J. Vac. Sci. Technol. A **6**, 1783 (1988).
[13] A. V. Palnichenko, A. M. Jonas, J.-C. Charller, A. S. Aronin, and J.-P. Issi, Nature (London) **402**, 162 (1999).
[14] A. C. Ferrari and J. Robertson, Phys. Rev. B **61**, 14095 (2000).
[15] B. R. Stoner, G.-H. M. Ma, S. D. Wolter, and J. T. Glass, Phys. Rev. B **19**, 11067 (1991).
[16] B.-R. Huang, C. H. Wu, and W. Z. Ke, Mater. Chem. Phys. **59**, 143 (1999).
[17] J. S. Lee, K. S. Liu, and I.-N. Li, Appl. Phys. Lett. **67**, 1555 (1995).
[18] W. J. Zhang, X. Jiang, and Y. B. Xia, J. Appl. Phys. **82**, 1896 (1997).

Downloaded 23 Aug 2010 to 133.68.192.97. Redistribution subject to AIP license or copyright; see http://jap.aip.org/about/rights_and_permissions